**Natural Hazards
and Earth System
Sciences**

Open Access

Discussions

Quantitative spatial analysis of rockfalls from road inventories: a combined statistical and physical susceptibility model

M. Böhme[1,2], M.-H. Derron[3], and M. Jaboyedoff[3]

[1]Geological Survey of Norway, Trondheim, Norway
[2]Norwegian University of Science and Technology, Trondheim, Norway
[3]Center for Research on Terrestrial Environment, University of Lausanne, Lausanne, Switzerland

Correspondence to: M. Böhme (martina.bohme@ngu.no)

NHESSD

2, 81–121, 2014

Quantitative spatial analysis of rockfalls from road inventories

M. Böhme et al.

Title Page

Abstract	Introduction
Conclusions	References
Tables	Figures

| ◄◄ | ►► |
| ◄ | ► |

Back | Close

Full Screen / Esc

Printer-friendly Version

Interactive Discussion

Abstract

Quantitative spatial analyses and statistical susceptibility assessments based on road inventories are often complicated due to the registration of impacts instead of source areas. A rockfall inventory from the Norwegian Directorate of Public Roads is analysed spatially in order to investigate potential controlling parameters in the Norwegian county Sogn and Fjordane. Quantitative spatial relationships are then used to model rockfall susceptibility with the help of the Weights-of-Evidence method. The controlling parameters tectono-stratigraphic position, quaternary geology, geological lineament density, relative relief and slope aspect resulted in the best performing model and thus yielded the basis for the statistical susceptibility map for the entire county of Sogn and Fjordane. Due to registered impacts instead of sources, the important parameter slope angle could not be included in the statistical models. Combining the statistical susceptibility model with a physically based model, restricts the susceptibility map to areas that are steep enough to represent a potential rockfall source. This combination makes it possible to use road inventories, with registered impacts instead of sources, for susceptibility modelling.

1 Introduction

Landslide inventories compiled by road authorities contain often the most comprehensive records, but are in many cases limited to registered impacts on the roads, lacking information about the source areas. This complicates quantitative spatial analyses of these inventories with respect to their controlling parameters depending on the resolution of the latter. Especially parameters originating from a digital elevation model (DEM), like slope angle, curvature, roughness or elevation itself, often have a resolution that is smaller than the distance between source and deposition area of landslides. Analysing the slope angle distribution for registered events of a road inventory, will in many cases yield too low slope angles. However, many studies indicate that a steep

slope is the principal pre-disposing factor for landslide processes especially rock slope failures (e.g., Aleotti and Chowdhury, 1999; Blais-Stevens et al., 2012; Erener and Düzgün, 2010; Kayastha et al., 2012b; Marzorati et al., 2002; Neuhäuser et al., 2012; Shirzadi et al., 2012). Quantitative spatial analyses result thus often in a susceptibility map reproducing a slope-angle map. On the other hand, a steep slope angle is a physical requirement for the presence of rock slope failures and using physically based approaches to define a relation between slope angle and the occurrence of landslides is thus much more appropriate. Hence, we propose an approach using a physical model to determine possible rockfall source areas and to update these source zones with relative susceptibilities obtained from a statistical model. This integration of statistically and physically based rockfall susceptibility models makes it possible to use road inventories with registered data points at deposits for the calculation of susceptibility maps.

The data basis of this study forms a rockfall inventory from the Norwegian Directorate of Public Roads. Rockfalls are a frequent hazard in Norway, especially within the Alpine topography of the coastal fjord areas. Steep slopes in combination with unfavourable climatic conditions, like heavy seasonal precipitation, intense snowmelt in spring and long frost periods, increase the vulnerability for rock slope failures in these regions (Blikra et al., 2006; Saintot et al., 2011). However, these might not be the single parameters controlling the spatial distribution of rockfalls. Jaboyedoff et al. (2005) give an overview on factors influencing rock slope instability, grouped into external and internal parameters. Various studies investigate rockfall locations with respect to their controlling parameters statistically (e.g., Duarte and Marquínez, 2002; Ruff and Czurda, 2008; Tanarro and Muñoz, 2012), or try to predict rockfall source areas by the means of different statistical or probabilistic modelling techniques on a regional scale, resulting in susceptibility maps (e.g., Blais-Stevens et al., 2012; Frattini et al., 2008; Marquínez et al., 2003; Marzorati et al., 2002; Shirzadi et al., 2012; Zahiri et al., 2006). However, the number of quantitative statistical susceptibility studies focusing specifically on rockfall is still very limited in comparison to those studying other landslide types or landslides in general, which has become very popular using GIS. Also Fell

Title Page

Abstract Introduction

Conclusions References

Tables Figures

|◄ ►|

◄ ►

Back Close

Full Screen / Esc

Printer-friendly Version

Interactive Discussion

et al. (2008) and van Westen et al. (2005) emphasize that it is necessary to study the susceptibility of different types of landslides separately due to the specific parameters controlling their failure mechanism.

Up to now studies of unstable rock slopes in Norway are mainly directed towards site-specific research of large instabilities (e.g., Böhme et al., 2011; Braathen et al., 2004), but not towards quantitative regional scale investigations. Only few studies discuss some more regional aspects of unstable rock slopes. For example, Blikra et al. (2006) describe a clustering of rockslides in specific zones of Norway, but do not include the underlying reasons in this spatial approach. Saintot et al. (2011) and Henderson and Saintot (2011) describe a link between rock slope instabilities in western Norway and ductile and brittle structures, but these studies are not based on quantitative analyses. Bjerrum and Jørstad (1968) and Sandersen et al. (1996) highlight a meteorological influence on rockfalls by applying simple binary statistics of historical events. In contrast, Dunlop (2010) investigated the relation between rock slope failures and meteorological conditions as well as topography and geology quantitatively applying Weights-of-Evidence based susceptibility mapping for a region in southwestern Norway (Hordaland and Sogn and Fjordane Counties). Furthermore, Erener and Düzgün (2010) present a statistically based susceptibility map of landslides for western Norway (Møre and Romsdal County) applying different regression methods. However, their focus is strongly on the mathematical methodology, and not on the input data and geological model. In addition, a lack of detailed knowledge about the local geological conditions as well as the used inventory is obvious.

The primary objective of this study is to determine the controlling parameters involved in the development of rockfalls in western Norway with the help of a quantitative spatial analysis. Furthermore, the possibility to use a road inventory with clear limitations for quantitative spatial analyses is investigated. Therefore the Weights-of-Evidence method is here first used as an explanatory tool, helping to quantify the relation between rockfalls and certain controlling parameters and second to produce a statistically based rockfall susceptibility map. The results provide a better understanding

of the spatial distribution of rockfalls in western Norway and the underlying reasons for their development. At last, the statistical susceptibility map is intersected with physically determined potential rockfall source zones (Derron, 2010) in order to obtain the final rockfall susceptibility map.

2 Study area

The study area comprises the entire county of Sogn and Fjordane, covering $18\,607\,\mathrm{km}^2$ of land area (Fig. 1). Historical data and geological studies show a high concentration of post-glacial gravitational slope failures as well as current rock slope instabilities in the Norwegian county Sogn and Fjordane, situated in western Norway (Blikra et al., 2006; Böhme et al., 2011; Saintot et al., 2011). This lead to several studies focusing on current rock slope instabilities in this county and geological knowledge about rock slope instabilities in these regions was largely extended (Böhme et al., 2011; Hermanns et al., 2011; Saintot et al., 2011).

The restriction to a county instead of using natural borders, the latter probably being more appropriate for modelling a natural process, was chosen due to the division of the Norwegian Directorate of Public Roads on a county base. In order to obtain the best possible homogeneity in the data, it is reasonable to use the limits of a county as the limits of the study area. Nevertheless, it is impossible to reach perfect homogeneity because of the subjective registration of rockfall events by different individuals.

3 Susceptibility assessment

Assuming that future landslides of any type will occur under similar geological and geometrical circumstances as past landslides of the same type have occurred, it is possible to study a landslide inventory in combination with several influencing factors and to analyse their spatial relation in order to prepare susceptibility maps (Guzzetti et al.,

1999). Various GIS-based statistical analysis methods as well as quantitative prediction models for landslide susceptibility or hazard have been proposed and applied in the literature. Introductions and overviews of quantitative statistical methods for landslide susceptibility or hazard assessment can be found in Brenning (2005); Chung and
⁵ Fabbri (2003); Guzzetti et al. (1999); Guzzetti (2005); Hervás and Bobrowsky (2009); Soeters and van Westen (1996) and van Westen (2000). New methods or modifications of existing ones are consistently developed or applied (e.g., Erener and Düzgün, 2010; Hasekioğulları and Ercanoglu, 2012; Kayastha et al., 2012a; Sezer et al., 2011). However, there is the tendency to more and more complicated mathematical models, that
¹⁰ are certainly powerful, but their physical significance is difficult to understand and those models tend to be black boxes for the standard user which makes it difficult to control the model (Leroi, 1996). With respect to quantitative statistical rockfall susceptibility prediction, namely discriminant analysis (Frattini et al., 2008), logistic regression (Marquínez et al., 2003; Marzorati et al., 2002; Shirzadi et al., 2012), Weights-of-Evidence
¹⁵ (Zahiri et al., 2006) and fuzzi logic (Blais-Stevens et al., 2012) have been applied. In this study the Weights-of-Evidence method is used to quantify the spatial relation between rockfalls and their controlling parameters in order to finally compute a susceptibility map for rockfalls in the county Sogn and Fjordane. Our focus is hereby not on the mathematical methodology and explains thus the usage of a mathematical relatively
²⁰ simple model.

3.1 Weights-of-Evidence method

The Weights-of-Evidence method was first applied to spatial geoscientific questions by Bonham-Carter et al. (1989). They combined spatial evidences for mineral deposits and produced predictive mineral potential maps. The Weights-of-Evidence method is
²⁵ a probabilistic method that uses known occurrences of a feature, termed as inventory within this study, to quantify spatial associations between these features and the controlling parameters that cause the features to occur (Bonham-Carter et al., 1989). Originally, the Weights-of-Evidence method was developed as a binary approach, but in this

study the extended Weights-of-Evidence method as introduced by Porwal et al. (2001) using multi-class controlling parameters was applied. The primary aim of the Weights-of-Evidence method is to weight and finally combine several controlling parameters, in order to get a prediction for the occurrence of a considered feature. However, in this study it is primarily used as an explanatory tool in order to investigate the spatial relations between rockfalls and their controlling parameters. The Weights-of-Evidence method has been widely applied for landslide studies (e.g., Armaş, 2012; Kayastha et al., 2012b; Lee et al., 2002; Neuhäuser et al., 2012; van Westen et al., 2003), but only limited for rockfalls explicitly (Zahiri et al., 2006).

Agterberg et al. (1990); Bonham-Carter et al. (1989) and Bonham-Carter (1994) give comprehensive descriptions of the mathematical formulation of the Weights-of-Evidence method. This method is well-known, and therefore only a basic introduction is given here.

In general, the Weights-of-Evidence method uses the theory of conditional probability, namely the rule of Bayes. It is based on the fact that the probability of an event, in this case a rockfall, will depend upon several circumstances. Weights are calculated for each controlling parameter class in order to quantify their strength of spatial influence on rockfall susceptibility, considering both the absence and presence of each controlling parameter class. Assuming that all rockfalls are known, probabilities can be estimated as simple volume proportions. The working formulas for calculating the weights are consequently the following:

$$W^+ = \ln\left(\frac{N\{R \cap X_i\}/N\{R\}}{N\{\overline{R} \cap X_i\}/N\{\overline{R}\}}\right) \tag{1}$$

$$W^- = \ln\left(\frac{N\{R \cap \overline{X_i}\}/N\{R\}}{N\{\overline{R} \cap \overline{X_i}\}/N\{\overline{R}\}}\right) \tag{2}$$

where $N\{R \cap X_i\}$ denotes the number of cells containing a rockfall event R and belonging to parameter class X_i. $\overline{R}$ and $\overline{X_i}$ indicate the absence of a rockfall or parameter class, respectively.

The calculated weights $W^{+/-}$ provide a measure of spatial association between the inventory and each controlling parameter class. A positive W^+ predicts that there are more rockfalls on that controlling parameter class than would occur pure randomly; conversely a negative W^+ predicts that fewer rockfalls occur than expected. The absolute value of the weights expresses how strong the spatial association between inventory and controlling parameter class is. The larger the absolute value, the stronger is the spatial association. A value of zero, or very close to zero, predicts that the rockfalls are distributed randomly with respect to that controlling parameter class.

In addition, the studentised contrast stud(C) serves as a measure about the statistical significance of the spatial association between the inventory and each controlling parameter:

$$\mathrm{stud}(C) = \frac{C}{\sigma(C)} \tag{3}$$

where the contrast $C = W^+ - W^-$ and $\sigma(C)$ is an approximation of the standard deviation of C, (see Agterberg et al., 1990 and Bonham-Carter et al., 1989 for its estimation). It is recommended that the modulus of the studentised contrast stud(C) should be larger than 2 for a significant spatial association (Bonham-Carter, 1994). Weights and studentised contrasts are calculated for each controlling parameter class based on the Weights-of-Evidence method with the help of the Esri ArcGIS toolbox "Spatial Data Modeller" (Sawatzky et al., 2009) and used to quantify the spatial relationship. The controlling parameters that have a significant spatial relation to the occurrence of rockfalls are selected and reclassified according to the analysis results in order to produce a susceptibility map. This reduction of classes is necessary in order to increase the statistical robustness of the weights (Bonham-Carter, 1994). The different controlling parameters can finally be combined based on the calculated weights assuming condi-

tional independence in between the parameters by updating the prior logit $\text{logit}\{R\}$ to the posterior logit:

$$\text{logit}\{R/X_1 \cap X_2 \cap \ldots X_n\} = \text{logit}\{R\} + \sum_{j=1}^{n} X_j^{+/-} \tag{4}$$

for $j = 1$ to n, where n is the total number of considered controlling parameters. "Logit" is defined as the natural logarithm of the ratio of the probability with that an event will occur to the probability that it will not occur. The posterior probability $P\{R/X_1 \cap X_2 \cap \ldots X_n\}$ or susceptibility can finally be obtained by back-transformation of the posterior logits into real probability values:

$$P\{R/X_1 \cap X_2 \cap \ldots X_n\} = \frac{e^{\text{logit}\{R/X_1 \cap X_2 \cap \ldots X_n\}}}{1 + e^{\text{logit}\{R/X_1 \cap X_2 \cap \ldots X_n\}}} \tag{5}$$

3.2 Validation of susceptibility maps and test of conditional independence

Success rate and prediction rate curves were used to evaluate the predictive power of the susceptibility map based on the time partition method as proposed by Chung and Fabbri (2003). In addition, the comparison of success rate curves from different susceptibility maps, based on different parameter combinations, has been used in order to select the best performing model. Success rate curves display how many of the analysed rockfalls are successfully detected by the susceptibility map. The steeper the curve, the better is the model efficiency.

The overall conditional independence was tested by comparing the number of observed rockfalls $N\{R\}$ to the number of predicted rockfalls $N\{R_p\}$. Given conditional independence, the number of both should be equal. Bonham-Carter (1994) suggests that the ratio $N\{R\}/N\{R_p\}$ should be > 0.85.

3.3 Combined statistical-physical susceptibility map

A rockfall susceptibility map has been previously produced for entire Norway separating between potential source areas and propagation zones (Derron, 2010). This map is based on a slope analysis method as proposed by Loye et al. (2009), resulting in
5 slope angle thresholds which are potentially unstable and could lead to rockfall. These thresholds depend on the slope angle, DEM cell size, type of bedrock and outcropping conditions. The main limitation of this rockfall susceptibility map is the limited resolution of the used DEM with a 25 m cell size. Small-sized rock cliffs can thus be missed during the detection of source cells. Furthermore, these maps are just displaying po-
10 tential source areas without any associated probability of rockfall release. The obtained probabilistic susceptibility map was thus used to update the rockfall source areas with a relative probability. At the same time, the probabilistic susceptibility map is with this step restricted to the potential source areas and includes thereafter only areas that are actually steep enough to cause rockfalls.

15 ## 4 Inventory

The national database of rapid mass movements in Norway is the result of joining four independent databases into one within the GeoExtreme project (Jaedicke et al., 2008, 2009). This database differentiates between five landslide types, namely rockslides, debris slides, snow avalanches, sub-aqueous slides and icefalls. The majority of regis-
20 tered landslides are from the Norwegian Directorate of Public Roads including all types of events that affected a road. For this study only events registered from the Norwegian Directorate of Public Roads within the category "ROCKSLIDE" and with a "RELEASE AREA" equal to "OPEN SLOPE" or "UNKNOWN" were extracted. Events in the category "ROCKSLIDE" represent almost exclusively rockfalls. In addition, points that are
25 located within tunnels have been eliminated. This results in an inventory containing 3259 rockfall events spanning a time period from 1973 until 2012 for the county of Sogn

and Fjordane. This dataset was divided into two subsets for validating the susceptibility map. The breakpoint was set to the end of the year 2002, because there was a reorganisation of the Norwegian Directorate of Public Roads incorporating changes in the division and potential changes in registration routines starting from 2003. Events older than this date were used as training data and events that occurred after the breakpoint are used as validation data.

There are several limitations applying for this database. It is a matter of course that all registered events are limited to public roads, but there is also no uniform registration of events along the public roads. The quality and completeness of data is strongly influenced by the internal division into road districts and personal abilities of the local observers. There exist no mandatory guidelines for the registration of events and whether an event will be registered or not depends basically on individuals. This results in a partially incomplete and biased database, both with respect to the area covered and to the time period investigated. In addition, registered locations are points where the rockfalls hit the road, but there exist no spatial information about the source area. In some cases, the registered points may even only be midpoints of a certain road section. However, it was not possible to obtain more detailed information about this conflict.

This study investigates rockfalls only spatially and temporal inconsistencies are thus not important. However, the severe spatial restrictions have been dealt with the following approaches. The first limitation, that the registrations are limited to public roads, has been solved by restricting the study area for the spatial analysis to a 1 km buffer around the road network, called training area in the following. The analysis results have then been used to predict rockfall susceptibility of the entire study area covering the complete county, assuming that the smaller training area is representative for the variability of the entire study area (Aleotti and Chowdhury, 1999; Dunlop, 2010; van Westen, 2000). The training area is covering 4290 km^2, corresponding to 3058 road km and the study area covers 18 607 km^2. On average there is 1 rockfall event per road km and 0.5 events per km^2 of the training area (Table 1).

The second limitation, the registered impacts on the road instead of the source areas will not have an effect for most geological information, since their resolution is lower than the distance between source and impact of a rockfall. For example the used geological maps have a scale of 1 : 250 000. This would mean that 1 mm on the map is equivalent to 250 m in the field. Dunlop (2010) defined the source areas of 98 rockslides recorded in the same database in a test area in Sogn and Fjordane. His results demonstrate that the average distance between source zone and impact on the road is 77 m, which is less than the resolution of most data used. However, major problems are expected analysing the DEM with a 25 m resolution and corresponding derivatives of it in the statistical analysis.

5 Parameters

A large set of potential controlling parameters has been spatially analysed with the help of the Weights-of-Evidence method. However, only the parameters that have most influence have been used for mapping the final susceptibility.

5.1 Bedrock geology

The bedrock of western Norway consists mainly of Lower Palaeozoic and Precambrian metamorphic rocks. The rocks of the study area have undergone intense reworking by a general NW–SE oriented crustal shortening during the Caledonian Orogeny, resulting in a thrust sheet transport towards SE onto the Precambrian basement (Roberts and Gee, 1985). The geological setting can be divided into three units, the Precambrian basement, the Caledonian nappes and Devonian sedimentary basins including a wide range of lithologies.

The basis for the geological parameters formed the 1 : 250 000 bedrock map of the Geological Survey of Norway (NGU Berggrunnskart). The original vector map was converted to a raster with 25 m cell size. Three different reclassifications were completed

based on (1) the rock type, (2) the tectono-stratigraphic position and (3) the metamorphic grade. The first reclassification is based on the relative competence of each rock type in the study area based on experience from fieldwork and is resulting in seven classes:

5   (1) Granular sedimentary rocks, plutonic rocks, felsic foliated rocks, mafic and ultramafic rocks, metamorphic rocks with low mechanical strength (like amphibolites, schists and micaschists), quartzite and marble (Fig. 2a)

    The second reclassification is founded on the fact that tectonic deformation, thus the tectonic weakening is higher in the nappes than in the basement. This classification

10   is not completely definite, since there exist different opinions about the affiliation of rock units to the different positions (Kildal, 1970; Ragnhildstveit and Helliksen, 1997; Sigmond, 1999; Solli and Nordgulen, 2008; Tveten et al., 1998). Therefore, different classifications have been analysed here and finally the classification displaying highest significance and largest weights has been used. The following tectono-stratigraphic

15   positions are represented in the study area:

    (2) Autochthon, lower allochthon, middle allochthon, upper allochthon, uppermost allochthon and Devonian sediments (Fig. 2b)

    The third reclassification with respect to the metamorphic grade is based on the geological map of the Fennoscandian Shield at a scale of 1 : 2 million (Koistinen et al.,

20   2001), resulting in four classes:

    (3) No, low, medium and high metamorphic grade (Fig. 2c)

5.2   Quaternary geology

In this study, the spatial relation in between the occurrence of rockfalls and landslide deposits as well as bare rock outcrops have been analysed (Fig. 2d). These features

25   were extracted from the quaternary map of the Geological Survey of Norway (NGU Løsmassekart), which is a mosaic of various scales, but mainly on a scale of 1 : 250 000 and 1 : 50 000 for the study area. The original vector map was used as a raster with 25 m cell size.

5.3 Tectonic structures

A significant amount of tectonic events affected the bedrock of western Norway, including the ductile Caledonian Orogeny, the semi-ductile post-orogenic collapse and also brittle tectonics, like the Permo-Triassic and Jurassic rifting phases; all together resulting in a high density of brittle, ductile and semi-ductile structures.

Two different sources of lineament maps have been available for this study:

– Geological lineaments from the bedrock map, mainly including thrusts and major faults at a scale of 1 : 250 000 (Fig. 2e and f; NGU Berggrunnskart).

– Geomorphological lineaments from Gabrielsen et al. (2002) based on satellite image (Landsat 7) interpretation at a scale of 1 : 750 000 (Fig. 2g and h).

All lineament maps were used in form of a density grid as well as a distance-to-closest-lineament grid, both with 25 m cell size.

5.4 Neotectonics

5.4.1 Present day uplift

Different geodetic data exhibit a high-rated present-day uplift in western Norway (Fjeldskaar et al., 2000; Kierulf et al., 2013; Olesen et al., 2000; Vestøl, 2006). Whereas the general trend of uplift is assumed to be a result of glacial isostasy, there exists a debate about the contribution of potential neotectonic processes (Bungum et al., 2010; Fjeldskaar et al., 2000; Olesen et al., 2000). Uplift and uplift gradient maps from Kierulf et al. (2013) have been used for statistical analysis (Fig. 2i and k).

5.4.2 Seismicity

Norway has a low to intermediate seismic intensity (Fjeldskaar et al., 2000). A concentration of earthquake activity is found west of mid-Norway, reflecting a rifted passive

continental margin (Bungum et al., 2000). The used earthquake catalogue, produced by NORSAR (Norwegian Seismic Array), is covering the time span from 1750 until 2007 (Dehls et al., 2000; Olesen et al., 2000). It contains 566 registered events with a magnitude $M_S \geq 2$ for western Norway and adjacent areas, whereof 6 events have a magnitude $M_S \geq 5$. In order to investigate the potential relation between earthquakes and rockfalls, earthquake density maps were calculated applying a search radius of 50 km and weighting each event with respect to its energy. Seismic energies E have been derived from magnitudes M_S based on the equation proposed by Gutenberg and Richter (2010):

$$\log E = 1.5 M_S + 11.8 \tag{6}$$

The earthquake density raster is mainly influenced by the earthquakes with $M_S \geq 4$ (Fig. 2l).

5.5 Topography and derived parameters

The topography of western Norway is strongly influenced by the quaternary glaciations. Coastal islands, long U-shaped valleys and many deep fjords with steep slopes are dominating landforms. This steep terrain in combination with heavily fractured exposed bedrock indicates that this area is susceptible to rockfall.

A digital elevation model with a cell size of 25 m forms the basis for different topographic parameters like slope angle, slope aspect, planar and profile curvature, roughness and relative relief (e.g. Fig. 2m and n). Slope angle, slope aspect and curvature are calculated with standard Esri ArcGIS procedures by fitting a plane to the elevation values of a 3 × 3 cell neighbourhood around the corresponding cell (Horn's method). The slope angle for this plane is calculated with the average maximum technique and the aspect is the direction the plane faces (Burrough and McDonnell, 1998). The curvature is the second derivative of the fitted plane. Local roughness has been assessed with the local standard deviation of the elevation values within a 9 × 9 moving window.

The relative relief has been calculated by determining the difference between minimum and maximum elevation within a moving circular window of 5 km radius.

5.6 Climate

The climate of western Norway displays large variations in between the coastal areas and the areas with high relief further inland. The coastal area of the study area includes the areas with the largest normal annual precipitation (3770 mm) as well as the highest normal annual temperatures (7.47 °C) of entire Norway. By contrast, the mountain areas, exhibit large areas with annual temperatures of −4 °C or less representing the lowest annual temperatures. The precipitation is essentially influenced by the large weather systems mainly coming from west, resulting in a zone of maximum precipitation along the coast and the mountain front.

Climatic normals of annual mean temperature and annual total precipitation for the period 1961–1990 were obtained from the Norwegian Meteorological Institute (Fig. 2o and p; Tveito et al., 2000).

6 Results of the spatial analysis

Ordered continuous parameters where classified in 40 equal classes for the spatial analysis. Weights (W^+ and W^-) and studentised contrasts stud(C) were calculated for all controlling parameters class-wise and for some parameters additionally cumulatively from lowest to highest class (ascending) and highest to lowest class (descending) (Fig. 3). These cumulative calculations allow defining a value where the parameters have no influence on rockfall anymore. The cumulative ascending weight calculation has been used for controlling parameters where low threshold values are expected to have a spatial influence on rockfalls, like the distance to lineaments. Cumulative descending weight calculation has been used for controlling parameters where high threshold values are expected, like seismicity, uplift, lineament density and precipita-

tion. All spatial analyses were done within the training area, thus within a road buffer of 1 km.

6.1 Bedrock geology

Analyses results of the bedrock geology indicate that only felsic foliated rocks have an increased susceptibility for rockfalls, whereas sedimentary rocks, metamorphic rocks with low mechanical strength, plutonic rocks and quartzite are significantly decreasing the susceptibility for rockfall (Table 2). However, the positive relations have only low weights in contrast to the negative relations, where a W^+ of −1.19 for sedimentary rocks is displaying one of the largest absolute values of the calculated weights for all parameters. Mafic and ultramafic rocks as well as marble have no significant relation to the occurrence of rockfalls. This is in contrast to Saintot et al. (2011), who claimed that metamorphic rocks with low mechanical strength as well as mafic and ultramafic rocks are particularly prone to rock slope failures. They observed that mafic and ultramafic rocks in western Norway are strongly weathered and highly fractured, yielding to larger numbers of rock slope instabilities. The positive relation of rockfalls to felsic foliated rocks may instead highlight that the structural control is larger than any lithological control on the development of rockfalls.

The analysis results of the tectono-stratigraphic positions indicate that only the middle allochthon has a significant positive relation with the occurrence of rockfalls (Table 2). The other units have all significant negative relations to the occurrence of rockfalls, except the uppermost allochthon. These results do not confirm the original assumption that the tectonic weakening, which is higher in the nappes than in the basement, may be a cause for higher rockfall activity.

Analysing the influence of the metamorphic grade on the occurrence of rockfalls yields a small positive relation to a high metamorphic grade and a negative relation to no, low and medium metamorphic grade (Table 2).

6.2 Quaternary geology

The spatial analysis of landslide deposits and bare rock outcrops with respect to the occurrence of rockfalls, exhibits a strong positive correlation of landslide deposits to rockfalls and a medium positive correlation of bare rock outcrops to rockfalls (Table 2). These results highlight the strong influence of the registered impacts on the road instead of the source areas. For registered source areas a larger positive correlation to bare rock than landslide deposits would be expected. However, present landslide deposits may highlight active rock cliffs and are thus yielding valuable information in order to define rockfall susceptibility.

6.3 Tectonic structures

Geologic lineament density indicates a positive spatial relation to the occurrence of rockfalls for high densities and a negative relation for low densities (Fig. 3a). In addition, the analysis exhibits less rockfalls in the vicinity of tectonic lineaments. Rockfalls occur preferentially within a distance of 1400 to 3800 m from a geological lineament. However, it is questionable if the lineaments can theoretically still have an influence on rock slope stability at those large distances. Theoretically an increasing lineament density or a closer distance to lineaments are assumed to cause a higher amount of fractures and subsequent an increased weathering, both reducing the rock strength (Ambrosi and Crosta, 2006; Brideau et al., 2005). The geomorphic lineament map displays no clear relation in between lineament density nor distance to lineaments and the occurrence of rockfalls.

6.4 Neotectonics

6.4.1 Present day uplift

The analyses of the uplift grid indicates a positive spatial relation to the occurrence of rockfalls for medium to high uplift values, but negative relations for low and very

Title Page

Abstract | Introduction

Conclusions | References

Tables | Figures

⏮ | ⏭

◀ | ▶

Back | Close

Full Screen / Esc

Printer-friendly Version

Interactive Discussion

high uplift values (Table 2, Fig. 3b). Regional uplift can theoretically be the cause for an increased relief and, therefore, may negatively affect the stability of rock slopes (Galadini, 2006; Martino et al., 2004). However, it remains unclear, which effect the amount of uplift has. The relation in between uplift gradient and the occurrence of rockfalls exhibits a negative relation for low uplift gradients and a positive relation for medium to high gradients (Table 2, Fig. 3c).

6.4.2 Seismicity

Seismicity may represent a potential trigger of rockfalls (e.g., Keefer, 1984; Marzorati et al., 2002) or may lead to rock mass strength reduction as a long term predisposing factor (Jaboyedoff et al., 2003). In the study area the seismicity on land is in general too low in order to trigger rockfalls (Keefer, 1984) and it should primarily be considered as a long term predisposing factor. However, the analysis results of earthquake density do not indicate any clear relation in between the location of rockfalls and earthquakes.

6.5 Topography

As described above the registered impacts on the road instead of the source areas cause major problems when analysing the DEM or derivatives of it, like resulting in positive spatial relations of rockfalls to low slope angles, planar or profile curvature around zero as well as low roughness values. Those properties can consequently not be used for describing relations to the occurrence of rockfall sources. However, the analyses of relative relief and slope aspect resulted in statistically and geologically significant spatial relations. Areas with a relative relief larger than 1020 m but smaller than 1620 m are prone to rockfalls, for areas with lower or higher relief the rockfall susceptibility is decreasing (Table 2, Fig. 3d). In addition, it can be demonstrated that a slope aspect from 206° to 332° (SW–NW) is prone to develop rockfalls, whereas other slope orientations have a negative relation to the occurrence of rockfalls (Table 2, Fig. 3e). A small positive correlation is also found for a slope aspect from 107 to 134° (ESE–SE). As described

above the climate in the study area is primarily influenced by large weather systems mainly coming from west. This results in a larger exposure of west-facing slopes to precipitation. However, this cannot be the only reason, since the spatial relation becomes less clear when analysing the general valley trends with a coarser grid. These slope orientations experience also the most intense melt water production, because of the combined favoured exposure to wind and solar radiation (Sandersen et al., 1996). On the other hand, Bjerrum and Jørstad (1968) and Sandersen et al. (1996) state that frost shattering is the most important factor for rockfalls in Norway. Diurnal freeze and thaw cycles are in general most effective on slopes facing SE to SW (Baillifard et al., 2004; Matsuoka and Sakai, 1999; Santi et al., 2009), however frost weathering of rocks depends on more factors than solely temperature and solar radiation (Matsuoka and Murton, 2008; Matsuoka, 2008).

6.6 Climate

A strong negative spatial correlation in between the occurrence of rockfalls and normal annual average temperatures lower than 0.5 °C has been identified. Higher temperatures, however, do not have any clear spatial relation to the occurrence of rockfalls.

Low normal annual total precipitation values are increasing the rockfall susceptibility, and very low values below 740 mm yr^{-1} as well as values above 1100 mm yr^{-1} have a negative relation to the occurrence of rockfalls (Fig. 3f). Sandersen et al. (1996) state that the precipitation is one of the most significant factors controlling rockfalls besides freeze-thaw cycles. However, this cannot be confirmed by analyzing normal annual values. It might be rather extreme events that have an influence on the development of rockfalls.

Title Page

Abstract   Introduction

Conclusions   References

Tables   Figures

⏮   ⏭

◀   ▶

Back   Close

Full Screen / Esc

7 Resulting susceptibility maps

Controlling parameters that have a clear and significant spatial relation to the occurrence of rockfalls were selected and regrouped into fewer classes, based on observed relations, so that the groups represent coherent relations with respect to the occurrence of rockfalls. Breakpoints that maximise the spatial association between rockfalls and controlling parameters and that are statistically significant have been identified based on calculated weights (W^+ and W^-) and studentised contrasts stud(C). The final classifications with the corresponding weights are summarized in Table 2. These controlling parameter maps were used to produce susceptibility maps based on the Weights-of-Evidence method for the training area. More than 50 different susceptibility maps with different parameter combinations were produced, testing the influence of each controlling parameter. Conditional independence was tested for all models and models where this assumption was violated were rejected. The model with the best performance was defined based on success rate curves and validated with a prediction rate curve (Fig. 4a). This model includes the controlling parameters tectono-stratigraphic position, quaternary geology, geological lineament density, relative relief and slope aspect and has an area under the success rate curve of 0.75. Success and prediction rate curves are very similar; however, it is noticeable that the success rate curve is slightly lower than the prediction rate curve. This is in general the opposite since the success rate curve is obtained using the data with that the model was calculated, whereas for the prediction rate curve the validation data is used, that has not been included for producing the model. It indicates that the validation data fits the model better than the training data. The prediction rate curve reveals that the model detects 70 % of rockfalls from the validation data set within 30 % of the training area.

Finally, a susceptibility map was calculated for the entire land area of the study area using the model obtained and validated within the training area (Fig. 5a). The final susceptibility map is characterized by in general lower susceptibilities close to the coast

and higher susceptibilities further inland. In addition, an increasing susceptibility from north to south can be observed.

Especially the entire inner fjord system of Sogne Fjord displays higher rockfall susceptibilities. At last the obtained susceptibility map was intersected with the source areas from the physically based rockfall susceptibility map (Fig. 5b and Fig. 6). The resulting susceptibility map is now restricted to areas that are steep enough to generate rockfalls. This is an important step, because the slope angle has not been included into the model so far. The physically determined rockfall source areas are now updated with relative probabilities.

8 Discussion

It has been questioned whether the existing slope failure inventory in Norway is suitable for statistical analysis or not because of its strong restrictions, mainly temporal and spatial discontinuity and incompleteness. However, temporal and spatial censoring of data is a problem that most inventories face including underreporting of data, incomplete data, inadequate sample time intervals or protective measures in high susceptible zones (Hungr et al., 1999). This study aimed to investigate the feasibility of statistic and probabilistic methods for analysing the inventories existing in Norway focusing on rock slope failures. The results confirm that the existing data in fact can be used to gain further knowledge about the controlling factors for rock slope failures in Norway based on statistical analysis in spite of strong restrictions. The results are robust with respect to changes of the study area as well as of the inventory and the restrictions have thus a limited influence. This study demonstrated the possibility of using road inventories for statistical analyses and should encourage for further analysis of the remaining inventory covering entire Norway in order to study regional variations within the controlling parameters.

Even if this study claims to be quantitative, a certain degree of subjectivity remains, when choosing the parameters for the final susceptibility map. Spatial relations of the

controlling parameters were judged based on expert knowledge whether they are geologically reasonable or not. Detailed geological knowledge about the study area is always required in order to be able to produce credible susceptibility maps. This small scale susceptibility map should be primarily used as a first order susceptibility map in order to detect hot spot areas, where critical factor combinations occur. More detailed investigations should be performed in areas that were identified as especially critical so that more precise susceptibility maps and additionally hazard maps can be prepared.

By replacing probabilities with relative frequencies it must be assumed that all rockfalls are known and the applied methods are thus strongly dependent on the completeness of the inventory (Schaeben, 2012). This is however assumed to be not the case for this study and will thus lead to an underestimation of the prior probability resulting in a bias of the weights as well as the final susceptibility (Agterberg and Cheng, 2002). Furthermore, the calculation of the susceptibility map with help of the Weights-of-Evidence method depends on the assumption of conditional independence. However, even if the tests for conditional independence do not reveal a strong violation of this assumption, a certain degree of conditional dependence will always be present in natural applications. Conditional dependence will lead to an overestimation of the final susceptibility. Based on our experience Weights-of-Evidence is a very powerful method for data exploration, but its application is limited for combining datasets to a susceptibility map due to the multiple assumption of conditional independence (Böhme, 2007; Schaeben, 2012). As logistic regression is closely related to Weights-of-Evidence, but not based on the assumption of conditional independence, this method yields a good alternative in generating susceptibility maps (Hosmer and Lemeshow, 2000). However, applying logistic regression with the same controlling parameters within the training area, results in a very similar susceptibility map as with the Weights-of-Evidence method, but in total with larger posterior probabilities. Success rate curves display that the results from both methods yield comparable predictabilities (Fig. 4a) and susceptibilities are thus most likely not over estimated by the Weights-of-Evidence method. Resulting posterior probabilities are in general very low with the highest posterior prob-

ability of 0.0027 for the source zones. For comparison, the prior probability for rockfalls in the study area is 0.0001 for each cell.

9 Conclusions

The spatial relationship between rockfall occurrence and potential controlling parameters in the county of Sogn and Fjordane has been evaluated using the Weights-of-Evidence method. Quaternary geology, tectono-stratigraphic position and geological lineament density have the strongest spatial relation to the occurrence of rockfalls in the study area (Table 2). A rockfall susceptibility map for the entire county of Sogn and Fjordane could be calculated based on the results of the statistical analyses of the controlling parameters. The model with best performance includes the controlling parameters tectono-stratigraphic position, quaternary geology, geological lineament density, relative relief and slope aspect. Combining the statistical susceptibility model with a physically based model restricts the susceptibility map to areas that are steep enough to represent a potential rockfall source. This combination makes it possible to use road inventories, with registered impacts instead of sources, for susceptibility modelling.

References

Agterberg, F. P. and Cheng, Q.: Conditional independence test for weights-of-evidence modeling, Natural Res. Res., 11, 249–255, 2002. 103
Agterberg, F. P., Bonham-Carter, G. F., and Wright, D. F.: Statistical pattern integration for mineral exploration, in: Computer Applications in Resource Estimation; Prediction and Assess-

ment for Metals and Petroleum, edited by: Gaal, G. and Merriam, D. F., 1–21, Pergamon Press, Oxford, New York, 1990. 87, 88

Aleotti, P. and Chowdhury, R.: Landslide hazard assessment: summary review and new perspectives, B. Eng. Geol. Environ., 58, 21–44, 1999. 83, 91

5 Ambrosi, C. and Crosta, G. B.: Large sackung along major tectonic features in the Central Italian Alps, Eng. Geol., 83, 183–200, 2006. 98

Armaş, I.: Weights of evidence method for landslide susceptibility mapping, Prahova Sub-carpathians, Romania, Nat. Hazards, 60, 937–950, 2012. 87

Baillifard, F., Jaboyedoff, M., Rouiller, J.-D., Robichaud, G., Locat, P., Locat, J., Couture, R.,
10 and Hamel, G.: Towards a GIS-based rockfall hazard assessment along the Quebec City Promontory, Quebec, Canada, in: Landslides: Evaluation and Stabilization, edited by: Lacerda, W. A., Ehrlich, M., Fontoura, A. B., and Sayão, A., 207–213, Taylor and Francis Group, London, 2004. 100

Bjerrum, L. and Jørstad, F. A.: Stability of Rock Slopes in Norway, Tech. Rep. NGI report no.
15 79, Norwegian Geotechnical Institute, Norway, 1968. 84, 100

Blais-Stevens, A., Behnia, P., Kremer, M., Page, A., Kung, R., and Bonham-Carter, G.: Landslide susceptibility mapping of the Sea to Sky transportation corridor, British Columbia, Canada: comparison of two methods, B. Eng. Geol. Environ., 71, 447–466, 2012. 83, 86

Blikra, L. H., Longva, O., Braathen, A., Anda, E., Dehls, J. F., and Stalsberg, K.: Rock slope
20 failures in Norwegian fjord areas: examples, spatial distribution and temporal pattern, in: Landslides from Massive Rock Slope Failure; NATO Science Series, IV. Earth and Environmental Sciences, vol. 49, edited by: Evans, S. G., Scarascia Mugnozza, G., Strom, A., and Hermanns, R. L., 475–496, Springer, Dordrecht, the Netherlands, 2006. 83, 84, 85

Böhme, M.: Predictive 3D Mineral Potential Modelling: Application to the VHMS Deposits of the
25 Noranda District, Canada, Diploma thesis, TU Bergakademie Freiberg, Germany, 2007. 103

Böhme, M., Saintot, A., Henderson, I., Henriksen, H., and Hermanns, R. L.: Rock-slope instabilities in Sogn and Fjordane County, Norway: a detailed structural and geomorphological analysis, in: Slope Tectonics, edited by: Jaboyedoff, M., 97–111, Geol. Soc. Spec. Publ., 351, London, 2011. 84, 85

30 Bonham-Carter, G. F.: Geographic Information Systems for Geoscientists: Modeling with GIS, Pergamon Press, Ontario, Canada, 1994. 87, 88, 89

Bonham-Carter, G. F., Agterberg, F. P., and Wright, D. F.: Weigths of evidence modeling: a new approach to mapping mineral potential, in: Statistical Applications in the Earth Sciences,

edited by: Agterberg, F. P. and Bonham-Carter, G. F., 171–183, Geological Survey of Canada, Canada, Report 89-09, 1989. 86, 87, 88

Braathen, A., Blikra, L. H., Berg, S. S., and Karlsen, F.: Rock-slope failure in Norway; type, geometry, deformation mechanisms and stability, Norw. J. Geol., 84, 67–88, 2004. 84

5 Brenning, A.: Spatial prediction models for landslide hazards: review, comparison and evaluation, Nat. Hazards Earth Syst. Sci., 5, 853–862, doi:10.5194/nhess-5-853-2005, 2005. 86

Brideau, M.-A., Stead, D., Kinakin, D., and Fecova, K.: Influence of tectonic structures on the Hope Slide, British Columbia, Canada, Eng. Geol., 80, 242–259, 2005. 98

Bungum, H., Lindholm, C., Dahle, A., Woo, G., Nadim, F., Holme, J., Gudmestad, O., Hagberg, T., and Karthigeyan, K.: New seismic zoning maps for Norway, the North Sea, and the United Kingdom, Seismol. Res. Lett., 71, 687–697, 2000. 95

Bungum, H., Olesen, O., Pascal, C., Gibbons, S., Lindholm, C., and Vestøl, O.: To what extent is the present seismicity of Norway driven by post-glacial rebound?, J. Geol. Soc. London, 167, 373–384, 2010. 94

15 Burrough, P. A. and McDonnell, R. A.: Principles of Geographic Information Systems, Oxford University Press, Oxford, 1998. 95

Chung, C.-J. F. and Fabbri, A. G.: Validation of spatial prediction models for landslide hazard mapping, Nat. Hazards, 30, 451–472, 2003. 86, 89

Dehls, J. F., Olesen, O., Bungum, H., Hicks, E. C., Lindholm, C. D., and Riis, F.: Neotectonic map: Norway and adjacent areas, 1 : 3 000 000, Geological Survey of Norway, Norway, 2000. 95

Derron, M.-H.: Method for the Susceptibility Mapping of Rock Falls in Norway, Tech. rep., Geological Survey of Norway, Norway, 2010. 85, 90, 120, 121

Duarte, R. M. and Marquínez, J.: The influence of environmental and lithologic factors on rockfall at a regional scale: an evaluation using GIS, Geomorphology, 43, 117–136, 2002. 83

Dunlop, S.: Rockslides in a changing climate: Establishing relationships between meteorological conditions and rockslides in southwestern Norway for the purposes of developing a hazard forecast system, Master thesis, Queen's University, Kingston, Canada, 2010. 84, 91, 92

30 Erener, A. and Düzgün, H. S. B.: Improvement of statistical landslide susceptibility mapping by using spatial and global regression methods in the case of Møre and Romsdal (Norway), Landslides, 7, 55–68, 2010. 83, 84, 86

Title Page

Abstract | Introduction

Conclusions | References

Tables | Figures

|◄ | ►|

◄ | ►

Back | Close

Full Screen / Esc

Printer-friendly Version

Interactive Discussion

Fell, R., Corominas, J., Bonnard, C., Cascini, L., Leroi, E., and Savage, W. Z.: Guidelines for landslide susceptibility, hazard and risk zoning for land use planning, Eng. Geol., 102, 85–98, 2008. 83

Fjeldskaar, W., Lindholm, C., Dehls, J. F., and Fjeldskaar, I.: Postglacial uplift, neotectonics and seismicity in Fennoscandia, Quaternary Sci. Rev., 19, 1413–1422, 2000. 94

Frattini, P., Crosta, G. B., Carrara, A., and Agliardi, F.: Assessment of rockfall susceptibility by integrating statistical and physically-based approaches, Geomorphology, 94, 419–437, 2008. 83, 86

Gabrielsen, R. H., Braathen, A., Dehls, J., and Roberts, D.: Tectonic lineaments of Norway, Norw. J. Geol., 82, 153–174, 2002. 94

Galadini, F.: Quaternary tectonics and large-scale gravitational deformations with evidence of rock-slide displacements in the Central Apennines (central Italy), Geomorphology, 82, 201–228, 2006. 99

Gutenberg, B. and Richter, C. F.: Magnitude and energy of earthquakes, Ann. Geophys.-Italy, 53, 7–12, 2010. 95

Guzzetti, F.: Landslide Hazard and Risk Assessment, Ph. D. thesis, Rheinische Friedrich-Wilhelms-Universität, Bonn, Germany, 2005. 86

Guzzetti, F., Carrara, A., Cardinali, M., and Reichenbach, P.: Landslide hazard evaluation: a review of current techniques and their application in a multi-scale study, Central Italy, Geomorphology, 31, 181–216, 1999. 85, 86

Hasekioğulları, G. D. and Ercanoglu, M.: A new approach to use AHP in landslide susceptibility mapping: a case study at Yenice (Karabuk, NW Turkey), Nat. Hazards, 63, 1157–1179, 2012. 86

Henderson, I. H. C. and Saintot, A.: Regional spatial variations in rockslide distribution from structural geology ranking: an example from Storfjord, western Norway, in: Slope Tectonics, edited by: Jaboyedoff, M., 79–95, Geol. Soc. Spec. Publ., 351, London, 2011. 84

Hermanns, R. L., Fischer, L., Oppikofer, T., Böhme, M., Dehls, J. F., Henriksen, H., Booth, A., Eilertsen, R., Longva, O., and Eiken, T.: Mapping of unstable and potentially unstable slopes in Sogn og Fjordane (work report 2008–2010), Tech. Rep. 2011.055, Geological Survey of Norway, Norway, 2011. 85

Hervás, J. and Bobrowsky, P.: Mapping: inventories, susceptibility, hazard and risk, in: Landslides – Disaster Risk Reduction, edited by: Sassa, K., and Canuti, P., 321–349, Springer, Berlin, 2009. 86

Quantitative spatial analysis of rockfalls from road inventories

M. Böhme et al.

Title Page

Abstract | Introduction

Conclusions | References

Tables | Figures

◄◄ | ►►

◄ | ►

Back | Close

Full Screen / Esc

Printer-friendly Version

Interactive Discussion

Hosmer, D. W. and Lemeshow, S.: Applied Logistic Regression, John Wiley and Sons, Inc., New York, 2nd edn., 2000. 103

Hungr, O., Evans, S., and Hazzard, J.: Magnitude and frequency of rock falls and rock slides along the main transportation corridors of southwestern British Columbia, Can. Geotech. J., 36, 224–238, 1999. 102

Jaboyedoff, M., Baillifard, F., and Derron, M.-H.: Preliminary note on uplift rates gradient, seismic activity and possible implications for brittle tectonics and rockslide prone areas: the example of western Switzerland, Bulletin de Géologie de l'Université de Lausanne, 88, 401–420, 2003. 99

Jaboyedoff, M., Baillifard, F., Derron, M.-H., Couture, R., Locat, J., and Locat, P.: Modular and evolving rock slope hazard assessment methods, in: Landslides and Avalanches: ICFL 2005 Norway, edited by: Senneset, K., Flaate, K., and Larsen, J. O., 187–194, Taylor and Francis Group, London, 2005. 83

Jaedicke, C., Solheim, A., Blikra, L. H., Stalsberg, K., Sorteberg, A., Aaheim, A., Kronholm, K., Vikhamar-Schuler, D., Isaksen, K., Sletten, K., Kristensen, K., Barstad, I., Melchiorre, C., Høydal, Ø. A., and Mestl, H.: Spatial and temporal variations of Norwegian geohazards in a changing climate, the GeoExtreme Project, Nat. Hazards Earth Syst. Sci., 8, 893–904, doi:10.5194/nhess-8-893-2008, 2008. 90

Jaedicke, C., Lied, K., and Kronholm, K.: Integrated database for rapid mass movements in Norway, Nat. Hazards Earth Syst. Sci., 9, 469–479, doi:10.5194/nhess-9-469-2009, 2009. 90

Kayastha, P., Dhital, M., and Smedt, F. D.: Application of the analytical hierarchy process (AHP) for landslide susceptibility mapping: a case study from the Tinau watershed, west Nepal, Comput. Geosci., 52, 398–408, 2012a. 86

Kayastha, P., Dhital, M. R., and Smedt, F. D.: Landslide susceptibility mapping using the weight of evidence method in the Tinau watershed, Nepal, Nat. Hazards, 63, 479–498, 2012b. 83, 87

Keefer, D. K.: Landslides caused by earthquakes, Geol. Soc. Am. Bull., 95, 406–421, 1984. 99

Kierulf, H. P., Ouassou, M., Simpson, M. J. R., and Vestøl, O.: A continuous velocity field for Norway, J. Geodesy, 87, 337–349, 2013. 94

Kildal, E. S.: Bedrock map Florø, 1 : 250 000, Geological Survey of Norway, 1970. 93

Koistinen, T., Stephens, M. B., Bogatchev, V., Nordgulen, Ø., Wenneström, M., and Korhonen, J.: Geological Map of the Fennoscandian Shield, 1 : 2 000 000, Geological Surveys of

Finland, Norway an Sweden and the North-West Department of Natural Resources of Russia, Russia, 2001. 93

Lee, S., Choi, J., and Min, K.: Landslide susceptibility analysis and verification using the Bayesian probability model, Environ. Geol., 43, 120–131, 2002. 87

5   Leroi, E.: Landslide hazard-risk maps at different scales: objectives, tools and developments, in: Proceedings of the 7th International Symposium on Landslides, Trondheim, edited by: Senneset, K., 17–21, Balkema, Rotterdam, 1996. 86

Loye, A., Jaboyedoff, M., and Pedrazzini, A.: Identification of potential rockfall source areas at a regional scale using a DEM-based geomorphometric analysis, Nat. Hazards Earth Syst. Sci., 9, 1643–1653, doi:10.5194/nhess-9-1643-2009, 2009. 90

10 Marquínez, J., Duarte, R. M., Farias, P., and Sánchez, M. J.: Predictive GIS-based model of rockfall activity in mountain cliffs, Nat. Hazards, 30, 341–360, 2003. 83, 86

Martino, S., Moscatelli, M., and Mugnozza, G. S.: Quaternary mass movements controlled by a structurally complex setting in the central Apennines (Italy), Eng. Geol., 72, 33–55, 2004. 99

15 Marzorati, S., Luzi, L., and Amicis, M. D.: Rock falls induced by earthquakes: a statistical approach, Soil Dyn. Earthq. Eng., 22, 565–577, 2002. 83, 86, 99

Matsuoka, N.: Frost weathering and rockwall erosion in the southeastern Swiss Alps: long-term (1994–2006) observations, Geomorphology, 99, 353–368, 2008. 100

Matsuoka, N. and Murton, J.: Frost weathering: recent advances and future directions, Permafrost Periglac., 19, 195–210, 2008. 100

20 Matsuoka, N. and Sakai, H.: Rockfall activity from an alpine cliff during thawing periods, Geomorphology, 28, 309–328, 1999. 100

Neuhäuser, B., Damm, B., and Terhorst, B.: GIS-based assessment of landslide susceptibility on the base of the weights-of-evidence model, Landslides, 9, 511–528, 2012. 83, 87

25 NGU Berggrunnskart: NGU Berggrunn – Nasjonal berggrunnsdatabase, available at: http://geo.ngu.no/kart/berggrunn/, 2013. 92, 94

NGU Løsmassekart: NGU Løsmasser – Nasjonal løsmassedatabase, available at: http://geo.ngu.no/kart/losmasse/, 2013. 93

Olesen, O., Dehls, J., Bungum, H., Riis, F., Hicks, E., Lindholm, C., Blikra, L. H., Fjeldskaar, W., 30 Olsen, L., and Longva, O.: Neotectonics in Norway, Final Report, Tech. Rep. 2000.002, Geological Survey of Norway, Norway, 2000. 94, 95

Porwal, A., Carranza, E. J. M., and Hale, M.: Extended weights-of-evidence modelling for predictive mapping of base metal deposit potential in Aravalli province, western India, Explor. Min. Geol., 10, 273–287, 2001. 87

Ragnhildstveit, J. and Helliksen, D.: Bedrock map Bergen, 1 : 250 000, Geological Survey of Norway, Norway, 1997. 93

Roberts, D. and Gee, D. G.: An introduction to the structure of the Scandinavian Caledonides, in: The Caledonide Orogen – Scandinavia and Related Areas, edited by: Gee, D. G. and Sturt, B. A., vol. 1, 55–68, John Wiley and Sons, Chichester, UK, 1985. 92

Ruff, M. and Czurda, K.: Landslide susceptibility analysis with a heuristic approach in the Eastern Alps (Vorarlberg, Austria), Geomorphology, 94, 314–324, 2008. 83

Saintot, A., Henderson, I., and Derron, M.-H.: Inheritance of ductile and brittle structures in the development of large rock slope instabilities: examples from western Norway, in: Slope tectonics, edited by: Jaboyedoff, M., 27–78, Geol. Soc. Spec. Publ., 351, London, 2011. 83, 84, 85, 97

Sandersen, F., Bakkehøi, S., Hestnes, E., and Lied, K.: The influence of meteorological factors on the initiation of debris flows, rockfalls, rockslides and rockmass stability, in: Proceedings of the 7th International Symposium on Landslides, Trondheim, edited by: Senneset, K., 97–114, Balkema, Rotterdam, 1996. 84, 100

Santi, P. M., Russell, C. P., Higgins, J. D., and Spriet, J. I.: Modification and statistical analysis of the Colorado Rockfall Hazard Rating System, Eng. Geol., 104, 55–65, 2009. 100

Sawatzky, D. L., Raines, G. L., Bonham-Carter, G. F., and Looney, C. G.: Spatial Data Modeller (SDM): ArcMAP 9.3 geoprocessing tools for spatial data modelling using weights of evidence, logistic regression, fuzzy logic and neural networks, http://www.ige.unicamp.br/sdm/ArcSDM93/, 2009. 88

Schaeben, H.: Comparison of mathematical methods of potential modeling, Math. Geosci., 44, 101–129, 2012. 103

Sezer, E. A., Pradhan, B., and Gokceoglu, C.: Manifestation of an adaptive neuro-fuzzy model on landslide susceptibility mapping: Klang valley, Malaysia, Expert Syst. Appl., 38, 8208–8219, 2011. 86

Shirzadi, A., Saro, L., Joo, O. H., and Chapi, K.: A GIS-based logistic regression model in rockfall susceptibility mapping along a mountainous road: Salavat Abad case study, Kurdistan, Iran, Nat. Hazards, 64, 1639–1656, 2012. 83, 86

Title Page

Abstract | Introduction

Conclusions | References

Tables | Figures

|◀ | ▶|

◀ | ▶

Back | Close

Full Screen / Esc

Printer-friendly Version

Interactive Discussion

Sigmond, E. M.: Bedrock map Odda, 1 : 250 000, Geological Survey of Norway, Norway, 1999. 93

Soeters, R., and van Westen, C. J.: Slope stability: recognition, analysis and zonation, in: Landslides Investigation and Mitigation, edited by: Turner, A. K. and Schuster, R. L., vol. Special Report 247, 129–177, Transportation Research Board, National Research Council, National Academy Press, Washington, DC, 1996. 86

Solli, A. and Nordgulen, Ø.: Bedrock map of Norway and the Caledonides in Sweden and Finland, 1 : 2 000 000, Geological Survey of Norway, Norway, 2008. 93

Tanarro, L. M., and Muñoz, J.: Rockfalls in the Duratón canyon, central Spain: inventory and statistical analysis, Geomorphology, 169–170, 17–29, 2012. 83

Tveito, O. E., Førland, E., Heino, R., Hanssen-Bauer, I., Alexandersson, H., Dahlström, B., Drebs, A., Kern-Hansen, C., Jónsson, T., Vaarby-Laursen, E., and Westman, Y.: Nordic temperature maps, Tech. Rep. 09/00 KLIMA, Norwegian Meteorological Institute, Norway, 2000. 96

Tveten, E., Lutro, O., and Thorsnes, T.: Bedrock map Ålesund, 1 : 250 000, Geological Survey of Norway, Norway, 1998. 93

van Westen, C. J.: The modelling of landslide hazards using GIS, Surv. Geophys., 21, 241–255, 2000. 86, 91

van Westen, C. J., Rengers, N., and Soeters, R.: Use of geomorphological information in indirect landslide susceptibility assessment, Nat. Hazards, 30, 399–419, 2003. 87

van Westen, C. J., Asch, T. W. J. V., and Soeters, R.: Landslide hazard and risk zonation – why is it still so difficult?, B. Eng. Geol. Environ., 65, 167–184, 2005. 84

Vestøl, O.: Determination of postglacial land uplift in Fennoscandia from leveling, tide-gauges and continuous GPS stations using least squares collocation, J. Geodesy, 80, 248–258, 2006. 94

Zahiri, H., Palamara, D., Flentje, P., Brassington, G., and Baafi, E.: A GIS-based weights-of-evidence model for mapping cliff instabilities associated with mine subsidence, Environ. Geol., 51, 377–386, 2006. 83, 86, 87

Title Page

Abstract | Introduction

Conclusions | References

Tables | Figures

|◀ | ▶|

◀ | ▶

Back | Close

Full Screen / Esc

Printer-friendly Version

Interactive Discussion

Table 1. Statistics about the rockfall events along the roads and within the training area.

Number of rockfall events	per road km	per km^2 of the training area
Minimum	0	0
Maximum	166	201
Average	1.05	0.54
Standard deviation	5.02	3.43

Table 2. Overview of classified controlling parameters used to calculate the susceptibility maps and their spatial association with the occurrence of rockfalls. In italics: parameter classes that are statistically not significant. In bold: controlling parameters that are included in the best performing susceptibility model.

Parameter	Parameter class	Area [km²]	Number of rockfalls	W^+	$\sigma(W^+)$	W^-	$\sigma(W^-)$	C	$\sigma(C)$	stud(C)
Rock type	Granular sedimentary rocks	257	50	−1.36	0.14	0.05	0.02	−1.41	0.14	−9.89
	Metamorphic rocks with low mechanical strength	905	533	-0.25	0.04	0.06	0.02	-0.31	0.05	-6.61
	Felsic foliated rocks	2296	2179	0.22	0.02	−0.34	0.03	0.56	0.04	15.08
	Plutonic rocks	657	426	−0.16	0.05	0.03	0.02	−0.18	0.05	−3.56
	Mafic and ultramafic rocks	*8*	*7*	*0.10*	*0.38*	*0.00*	*0.02*	*0.10*	*0.38*	*0.26*
	Marble	*1*	*0*	*0.00*	*0.00*	*0.00*	*0.00*	*0.00*	*0.00*	*0.00*
	Quartzite	165	64	−0.67	0.13	0.02	0.02	−0.69	0.13	−5.49
Tectono-stratigraphic position	Lower allochton	1463	704	−0.46	0.04	0.17	0.02	−0.63	0.04	−14.81
	Middle allochton	1028	1450	0.62	0.03	−0.31	0.02	0.93	0.04	26.50
	Upper allochton	155	87	−0.30	0.11	0.01	0.02	−0.31	0.11	−2.85
	Uppermost allochton	*15*	*8*	*-0.36*	*0.35*	*0.00*	*0.02*	*-0.36*	*0.35*	*-1.01*
	Devonian sediments	254	46	−1.43	0.15	0.05	0.02	−1.48	0.15	−9.97
	Autochthon	1376	964	−0.08	0.03	0.04	0.02	−0.12	0.04	−3.05
Metamorphic grade	No	425	197	−0.49	0.07	0.04	0.02	−0.54	0.07	−7.28
	Low	572	204	−0.76	0.07	0.08	0.02	−0.83	0.07	−11.54
	Medium	155	87	−0.30	0.11	0.01	0.02	−0.31	0.11	−2.85
	High	3134	2771	0.15	0.02	−0.59	0.05	0.74	0.05	15.08
Quaternary geology	Landslide deposits	489	905	0.89	0.03	−0.20	0.02	1.10	0.04	27.99
	Bare rock	1709	1618	0.22	0.02	−0.18	0.02	0.40	0.04	11.37
	Others	2092	736	−0.77	0.04	0.41	0.02	−1.18	0.04	−28.24
Geological lineament density	0.039–0.447 km⁻²	2269	1023	−0.52	0.03	0.38	0.02	−0.90	0.04	−23.78
	0.447–0.812 km⁻²	1991	2182	0.37	0.02	−0.48	0.03	0.85	0.04	22.82
	0.812–0.898 km⁻²	30	54	0.86	0.14	−0.01	0.02	0.87	0.14	6.30
Uplift	2.09–3.15 mm yr⁻¹	3034	1534	−0.41	0.03	0.60	0.02	−1.01	0.04	−28.77
	3.15–4.11 mm yr⁻¹	1129	1714	0.69	0.02	−0.44	0.03	1.13	0.04	32.33
	4.11–4.33 mm yr⁻¹	118	11	−2.10	0.30	0.02	0.02	−2.13	0.30	−7.04
Uplift gradient	0.0002–0.0006°	1406	654	−0.49	0.04	0.17	0.02	−0.66	0.04	−15.17
	0.0006–0.0024°	2885	2605	0.17	0.02	−0.49	0.04	0.66	0.04	15.17
Relative relief	45–1020 m	2125	901	−0.58	0.03	0.36	0.02	−0.94	0.04	−24.08
	1020–1620 m	1911	2229	0.43	0.02	−0.56	0.04	0.99	0.04	26.31
	1620–2217 m	255	129	−0.41	0.09	0.02	0.02	−0.43	0.09	−4.75
Slope aspect	0–107°	1404	636	−0.52	0.04	0.18	0.02	−0.70	0.04	−15.75
	107–134°	263	240	0.19	0.06	−0.01	0.02	0.20	0.07	2.96
	134–206°	950	640	−0.12	0.04	0.03	0.02	−0.15	0.04	−3.43
	206–332°	1348	1545	0.41	0.03	−0.27	0.02	0.68	0.04	19.29
	332–359°	326	198	−0.22	0.07	0.02	0.02	−0.24	0.07	−3.26
Normal annual total precipitation	500–741 mm yr⁻¹	157	46	−0.95	0.15	0.02	0.02	−0.98	0.15	−6.58
	741–1143 mm yr⁻¹	624	1337	1.04	0.03	−0.37	0.02	1.41	0.04	39.46
	1143–3713 mm yr⁻¹	3500	1876	−0.35	0.02	0.84	0.03	−1.20	0.04	−33.73

Discussion Paper | Discussion Paper | Discussion Paper | Discussion Paper

NHESSD

2, 81–121, 2014

Quantitative spatial analysis of rockfalls from road inventories

M. Böhme et al.

Title Page

Abstract   Introduction

Conclusions   References

Tables   Figures

◀   ▶

◀   ▶

Back   Close

Full Screen / Esc
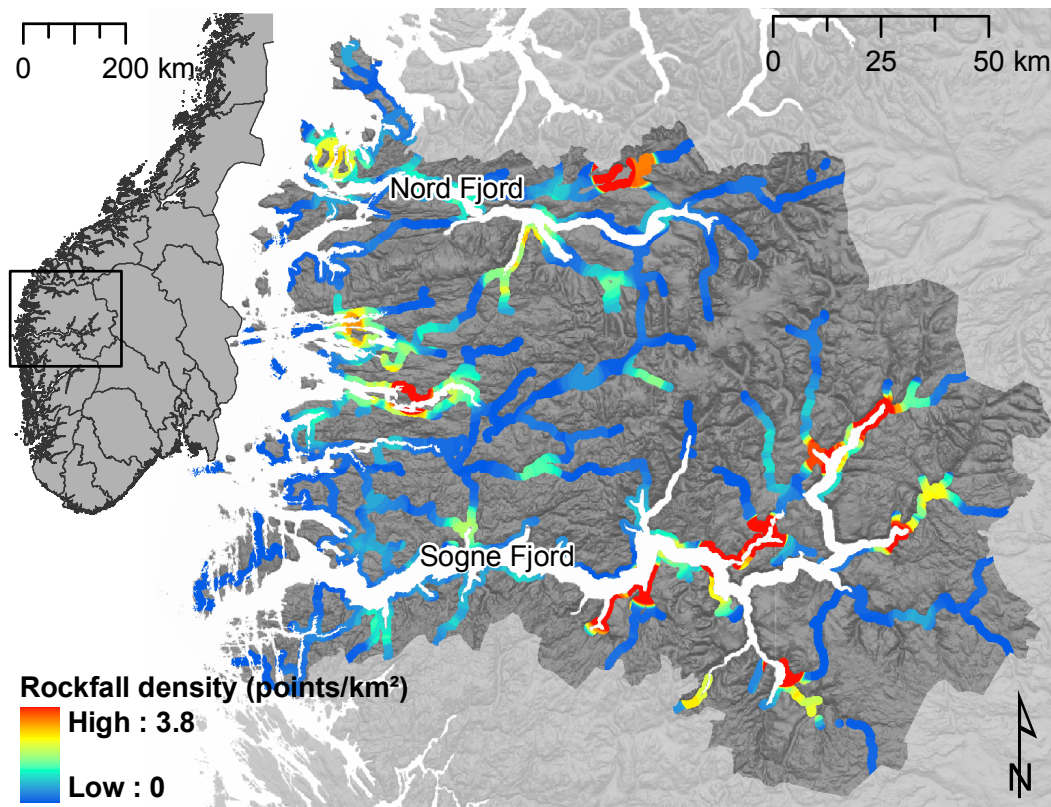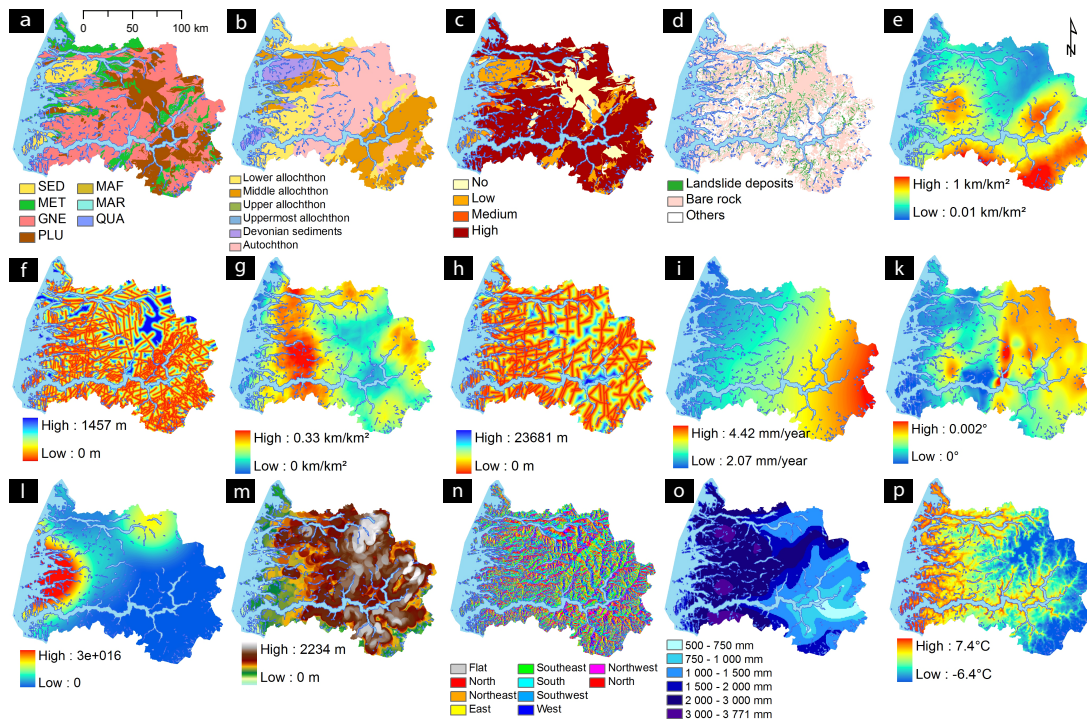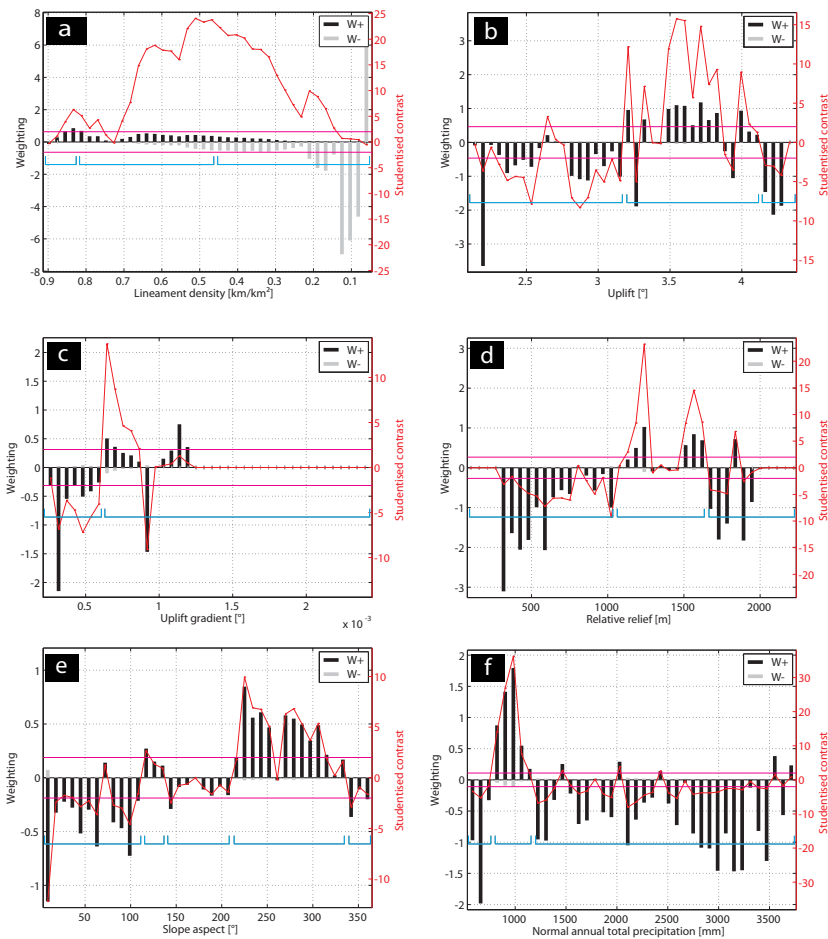
Printer-friendly Version

Interactive Discussion

Fig. 1. Overview of the study area, Sogn and Fjordane County, displaying the rockfall density within a road buffer of 1 km. This road buffer forms the limit of the training area used for statistical analyses. The inset shows the location of the study area within Norway.

Fig. 2. Caption on next page.

Fig. 2. Overview of analysed parameters. **(a)** Rock type (SED: granular sedimentary rocks, MET: metamorphic rocks with low mechanical strength, GNE: felsic foliated rocks, PLU: plutonic rocks, MAF: mafic and ultramafic rocks, MAR: marble, QUA: quartzite); **(b)** tectono-stratigraphic position; **(c)** metamorphic grade; **(d)** quaternary geology; **(e)** geological lineament density; **(f)** distance to geological lineaments; **(g)** geomorphological lineament density; **(h)** distance to geomorphological lineaments; **(i)** uplift; **(k)** uplift gradient; **(l)** earthquake density; **(m)** relative relief; **(n)** slope aspect; **(o)** normal annual total precipitation for the period 1961–1990; **(p)** normal annual mean temperature for the period 1961–1990.

Fig. 3. Caption on next page.

Fig. 3. Examples for results of the spatial analysis with the Weights-of-Evidence method. All continuous parameters have been reclassified into 40 classes each. Weights (W^+ and W^-) and studentised contrast stud(C) have been calculated for each class seperately **(b–f)** or with cumulative descending **(a)** or ascending classes in order to obtain the spatial relation of each class to the occurrence of rockfalls. Horizontal pink lines mark |stud(C)| = 2, thus all studentised contrast values above or below have a significant spatial relation. The final classifications are indicated by blue brackets. **(a)** Geological lineament density (cumulative descending classes). Local maxima of stud(C) are used as breakpoints for the final reclassification. All classes right of the maximal stud(C) have a negative association to the occurrence of rockfalls, resulting in decreasing W^+ and stud(C). **(b)** Uplift. No clear peaks, but in general a positive relation for medium to high uplift. **(c)** Uplift gradient. One distinct positive peak at low uplift gradient is displayed. **(d)** Relative relief. Weights exhibit two major positive peaks. **(e)** Slope aspect. A clear positive relation for slopes facing SW–NW can be observed. **(f)** Normal annual total precipitation. One major positive peak for low precipitation values can be observed.
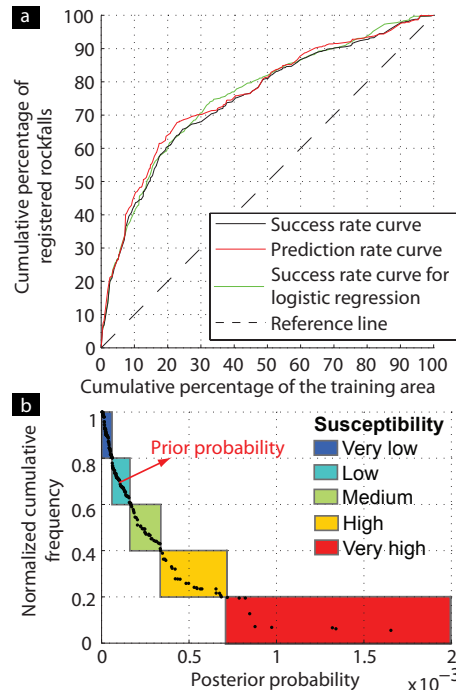
Fig. 4. (a) Success rate and prediction rate curve for the best performing Weights-of-Evidence model as well as success rate curve for logistic regression model using the same parameters as the Weights-of-Evidence model. All three curves are very similar. **(b)** Distribution of the posterior probability for all registered rockfalls. 70 % of the rockfalls have a posterior probability larger than the prior probability of 0.0001. Posterior probabilities are classified into five susceptibility classes, indicated by coloured boxes, based on equally percentages of registered rockfalls for each class. Each susceptibility class contains 20 % of the registered rockfalls.
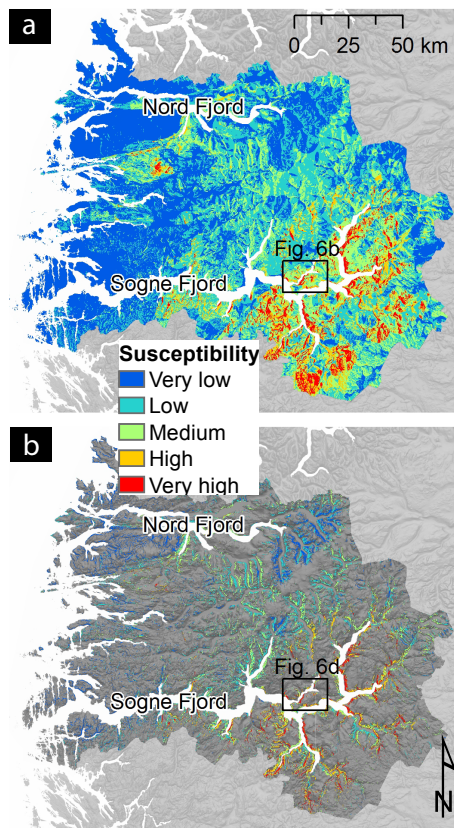
Fig. 5. Resulting susceptibility maps based on the controlling parameters tectono-stratigraphic position, quaternary geology, geological lineament density, relative relief and slope aspect. **(a)** Susceptibility for the entire land area and **(b)** for the physically determined source zones from Derron (2010).
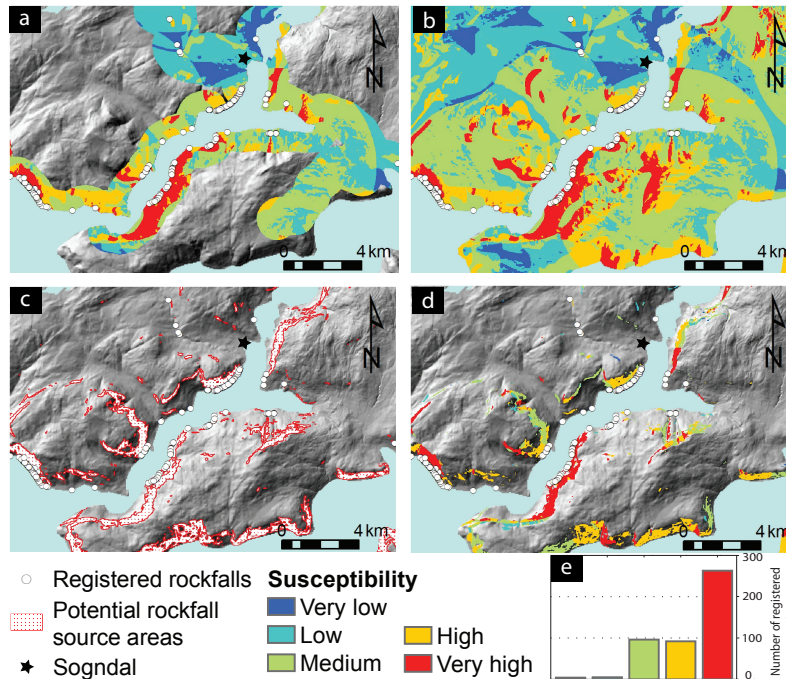
Fig. 6. Detail of the different susceptibility maps. For the location see Fig. 5. **(a)** Susceptibility within a road buffer of 1 km, which has been used as training area for analyzing the spatial relation between rockfalls and controlling parameters as well as for validation of the model. **(b)** Susceptibility for the entire land area based on the model set up from **(a)**. **(c)** Rockfall susceptibility map based on Derron (2010). **(d)** Combined rockfall susceptibility map displaying the physically determined source zones from Derron (2010) updated with probabilistically assessed susceptibilities. **(e)** Distribution of susceptibility for the registered rockfalls within the displayed area.